H_∞ Gain-scheduled Controller Design for Rejection of Time-varying Narrow-band Disturbances Applied to a Benchmark Problem

Alireza Karimi*, Zlatko Emedi[1]

Laboratoire d'Automatique, Ecole Polytechnique Fédérale de Lausanne, CH-1015 Lausanne, Switzerland.

Abstract

A new method for H-infinity gain-scheduled controller design by convex optimization is proposed that uses only frequency-domain data. The method is based on loop shaping in the Nyquist diagram with constraints on the weighted infinity-norm of closed-loop transfer functions. This method is applied to a benchmark for adaptive rejection of multiple narrow-band disturbances. First, it is shown that a robust controller can be designed for the rejection of a sinusoidal disturbance with known frequency. The disturbance model is fixed in the controller, based on the internal model principle, and the other controller parameters are computed by convex optimization to meet the constraints on the infinity-norm of sensitivity functions. It is shown next that a gain scheduled-controller can be computed for a finite set of disturbance frequencies by convex optimization. An adaptation algorithm is used to estimate the disturbance frequency which adjusts the parameters of the internal model in the controller. The simulation and experimental results show the good performance of the proposed control system.

Keywords: Gain-scheduled control, robust control, H_∞ control, Adaptive disturbance rejection, active suspension system

1. Introduction

In control engineering problems, disturbance rejection is an extremely important task. Some disturbances have periodic character and can even be expressed as combination of few sinusoidal signals. Typical examples of systems with periodic disturbances are hard disks [10], optical disk drives [1], helicopter rotor blades [17] and active noise control systems [19].

In the case that the disturbance frequency is known, certain approaches, such as internal model control and repetitive control techniques can be applied. If unknown frequency can be measured directly or indirectly, which happens e.g. in some active noise control applications, adaptive feedforward control can be used for the rejection of disturbance. In [14], it was shown that the standard adaptive feedforward control algorithm is equivalent to the internal model control law. Survey on methods in both cases of known and unknown disturbance frequency can be found in [2].

Since it is not always possible to measure the disturbance frequency with a transducer, the parameter estimation methods are often used to estimate the parameters of the disturbance model. Therefore, almost all unknown disturbance rejection algorithms generally lead to a *direct* or *indirect* adaptive implementation, which can be referred to as "adaptive regulation". The reason is that the controller parameters are adapted with respect to variations of parameters of the disturbance model. In [8], two approaches are compared on an active suspension system. The first approach is a direct adaptive control scheme with Q-parameterization of the controller, where the disturbance is rejected by adjusting the parameters of the Q polynomial. The second approach is an indirect adaptive control because the disturbance model is estimated first and then, based on the internal model principle, new controller is calculated to reject the disturbance.

A linear parameter-varying (LPV) controller design method is described in [7] for rejection of sinusoidal disturbances. In this approach, an LPV controller is designed with H_∞ performance based on the method proposed in [5] and [16], using a single quadratic Lyapunov function for all values of measured frequency. Discrete-time state-space state-feedback and full-order output feedback LPV controller design methods are described in [20] and [18], guaranteeing closed-loop stability for infinitely fast variations of disturbance frequencies using a single Lyapunov matrix over the whole scheduling parameter space. A new method for fixed-order LPV controller design with application to disturbance rejection of an active suspension system is proposed in [21].

In this paper, a fixed-order H_∞ gain-scheduled controller design method based only on the frequency-domain

*Corresponding author

Email addresses: alireza.karimi@epfl.ch (Alireza Karimi), zlatko.emedji@epfl.ch (Zlatko Emedi)

[1]This research work is financially supported by the Swiss National Science Foundation under Grant No. 200021-121749.

data is proposed. In this method, computation of the controller parameters and their interpolation are performed by one convex optimization. Moreover, a solution to a challenging benchmark problem [9] for rejection of time-varying narrow-band disturbances is provided. The results are computed using a new public-domain toolbox for robust controller design in the frequency domain which is available in [11].

The advantages of the proposed method with respect to the LPV controller design methods are:

- There is no need for a parametric model of the plant and the frequency response can be used directly for controller design. As a result, the approach can be used for discrete- continuous-time systems with pure time delay.
- The controller order is fixed that allows less computation effort in real-time applications.
- Since the stability and performance are guaranteed for frozen scheduling parameters, the method has less conservatism with respect to LPV controllers based on quadratic stability.

The last item can be considered as a drawback as well, because the stability and performance are not guaranteed for fast variations of the scheduling parameters. The other drawbacks are the limitation of the controller structure to linearly parameterized controllers and the dependence of the final solution on the choice of the desired open-loop transfer function L_d. Some propositions to overcome these drawbacks are given in [12].

The proposed method, like the other adaptive methods used in the benchmark, guarantees the stability and performance only for frozen and slowly time-varying scheduling parameters. However, in practice, as it is shown for the benchmark problem, the designed controllers stabilize the system even for rather fast variations.

The paper is organized as follows: Section 2 describes the gain-scheduled H_∞ controller design method that uses only the frequency response of the model. The method is applied to the benchmark problem for adaptive disturbance rejection of an active suspension system in Section 3. Section 4 presents the simulation and the experimental results. Finally, Section 5 gives some concluding remarks.

2. Gain-scheduled H_∞ controller design

A fixed-order H_∞ controller design method for spectral models is proposed in [12]. In this section we extend this method to design of gain-scheduled H_∞ controllers.

A classical way to design gain-scheduled controllers includes two steps:

1. A set of controllers are designed for each operating point (if the operating points are a continuous function of a scheduling parameter, a fine grid is used to obtain a finite set).
2. The controller parameters are interpolated by a polynomial function of the scheduling parameter.

In order to reduce the complexity of the gain-scheduled controller, a linear or low-order interpolation is normally used. In this case, the stability and performance are not necessarily preserved even for the gridded scheduling parameter. The method that we propose puts these two steps together and computes a gain-scheduled controller that satisfies the stability and H_∞ performance conditions for all gridded values of the scheduling parameter using the convex optimization methods. For the ease of presentation, a scalar scheduling parameter and one H_∞ constraint on the weighted sensitivity function are considered. The extension to vector of scheduling parameters and H_∞ constraints on several sensitivity functions is straightforward. In the sequel, the class of models, controllers and design specifications are defined and a convex optimization problem is proposed that results in a gain-scheduled controller.

2.1. Class of models

The class of causal discrete-time LTI-SISO models with bounded infinity-norm is considered. It is assumed that the spectral model of the system as a function of the scheduling parameter θ, $G(e^{-j\omega}, \theta)$ is available. The bounded infinity norm condition will be relaxed later on to consider systems with poles on the unit circle. Since only the frequency-domain data are used in the design method the extension to continuous-time systems is straightforward (see [12]).

2.2. Class of controllers

Linearly parameterized discrete-time gain-scheduled controllers are considered:

$$K(z^{-1}, \rho(\theta)) = \rho^T(\theta)\phi(z^{-1}), \tag{1}$$

where

$$\phi^T(z^{-1}) = [\phi_1(z^{-1}), \phi_2(z^{-1}), \ldots, \phi_n(z^{-1})] \tag{2}$$

represents the vector of n stable transfer functions, namely basis functions vector that may be chosen from a set of generalized orthonormal basis functions, e.g. Laguerre basis [15], and

$$\rho^T(\theta) = [\rho_1(\theta), \rho_2(\theta), \ldots, \rho_n(\theta)] \tag{3}$$

represents the vector of controller parameters. The dependence of the controller parameters ρ_i to θ can be affine or polynomial, e.g. $\rho_i(\theta) = \rho_{i_0} + \rho_{i_1}\theta + \cdots + \rho_{i_{n_\theta}}\theta^{n_\theta}$.

The main reason to use a linearly parameterized controller is that every point on the Nyquist diagram of the open-loop transfer function becomes a linear function of the vector of controller parameters $\rho(\theta)$:

$$\begin{aligned} L(e^{-j\omega}, \rho(\theta)) &= K(e^{-j\omega}, \rho(\theta))G(e^{-j\omega}, \theta) && (4)\\ &= \rho^T(\theta)\phi(e^{-j\omega})G(e^{-j\omega}, \theta), && (5) \end{aligned}$$

that helps obtaining a convex parameterization of fixed-order H_∞ controllers.

2.3. Design specifications

The nominal performance can be defined by (see [4])

$$\|W_1 S(\rho(\theta))\|_\infty < 1 \qquad \forall\theta, \tag{6}$$

where $S(z^{-1}, \rho(\theta)) = [1 + L(z^{-1}, \rho(\theta))]^{-1}$ is the sensitivity function and W_1 represents the performance weighting filter. The approach proposed in [12] is based on the linearization of this constraint around a known desired open-loop transfer function L_d (that may be a function of θ as well). The main interest of this linearization is that it gives not only sufficient conditions for the nominal performance but also some conditions on L_d that guarantee the stability of the closed-loop system. The linear constraints are given by [12]:

$$\begin{aligned} &|W_1(e^{-j\omega})[1 + L_d(e^{-j\omega}, \theta)]| - \\ &R_e\{[1 + L_d(e^{j\omega}, \theta)][1 + L(e^{-j\omega}, \rho(\theta))]\} < 0, \forall\omega, \forall\theta \end{aligned} \tag{7}$$

It is easy to show that the inequality in (6) is met if the above inequality is satisfied. Knowing that the real value of a complex number is always less than or equal to its absolute value, we have:

$$\begin{aligned} &|W_1(e^{-j\omega})[1 + L_d(e^{-j\omega}, \theta)]| - \\ &\quad |1 + L_d(e^{j\omega}, \theta)||1 + L(e^{-j\omega}, \rho(\theta))| < 0, \forall\omega, \forall\theta \end{aligned} \tag{8}$$

which leads to

$$|W_1(e^{-j\omega})| < |1 + L(e^{-j\omega}, \rho(\theta))|, \quad \forall\omega, \forall\theta \tag{9}$$

that is equivalent to (6). Moreover, it can be shown that the number of encirclements of the critical point by L and L_d is equal. As a result, the closed-loop stability is ensured if $L_d(\theta)$ satisfies the Nyquist criterion for all θ (e.g. it does not turn around -1 for stable plant models). On the other hand, if the plant model and/or the controller have unbounded infinity-norm, i.e. the poles on the unit circle, these poles should be included in L_d (see [12]).

The graphical interpretation of this method is given in Fig.1. It is well known that the H_∞ performance condition in (6) is satisfied if and only if there is no intersection between $L(e^{-j\omega}, \rho(\theta))$ and a circle centered at -1 with radius $|W_1(e^{j\omega})|$ [4]. It is clear that this condition is satisfied if $L(e^{-j\omega}, \rho(\theta))$ lies at the side of d that excludes -1 for all ω and θ, where d is tangent to the circle and orthogonal to the line connecting -1 to $L_d(e^{-j\omega}, \theta)$. The conservatism of the proposed approach depends on the choice of L_d and discussed in [12]. It is clear that if $L_d = L$ there is no conservatism. Therefore, choosing L_d as close as possible to L will reduce significantly this conservatism. Since L is not a priori known, an iterative approach can be used to reduce the conservatism (at each iteration L of the previous iteration is used as L_d).

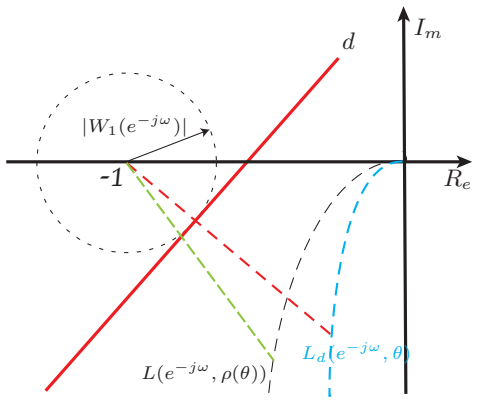

Figure 1: Linear constraints for robust performance

2.4. Optimization problem

The constraints in (7) should be satisfied for all $\omega \in [0, \omega_n]$, where ω_n is the Nyquist frequency, and for all $\theta \in [\theta_{\min}, \theta_{\max}]$. This leads to an infinite number of constraints that is numerically intractable. A practical approach is to choose finite grids for ω and the scheduling parameter θ and find a feasible solution for the grid points. This leads to a large number of linear constraints that can be handled efficiently by linear programming solvers. By increasing the number of scheduling parameters, the number of constraints will increase drastically that increases the optimization time. In this case a scenario approach can be used that guarantees the satisfaction of all constraints with a probability level when they are only satisfied for a finite number of randomly chosen scheduling parameters [3]. Some of the effects of gridding in frequency and additional constraints that can be imposed for ensuring good behavior between the grid points are described in [6].

3. Active Suspension Benchmark

The objective of the benchmark is to design a controller for the rejection of unknown/time-varying multiple narrow band disturbances located in a given frequency region. The proposed controllers will be applied to the active suspension system of the Control Systems Department in Grenoble (GIPSA - lab) [9]. The block diagram of the active suspension system together with the proposed gain scheduled controller is shown in Fig. 2.

The system is excited by a sinusoidal disturbance $v_1(t)$ generated using a computer-controlled shaker, which can be represented as a white noise signal, $e(t)$, filtered through the disturbance model H. The transfer function G_1 between the disturbance input and the residual force in open-loop, $y_p(t)$, is called the primary path. The signal $y(t)$ is a measured voltage, representing the residual force, affected by the measurement noise. The secondary path is the transfer function G_2 between the output of the controller $u(t)$ and the residual force in open-loop. The control

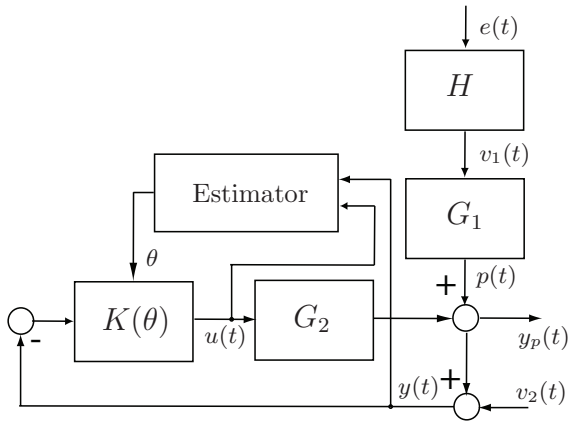

Figure 2: Block diagram of the active suspension system

input drives an inertial actuator through a power amplifier. The sampling frequency for both identification and control is 800Hz, as chosen by the benchmark organisers.

The disturbance consists of one to three sinusoids, leading to three levels of benchmark depending on the number of sinusoids. Disturbance frequencies are unknown but lie in an interval from 50 to 95Hz. The controller should reject the disturbance as fast as possible. We explain in detail the control structure and the design method for Level 1. The extension to the other levels is straightforward.

3.1. Controller design for Level 1

An H_∞ gain-scheduled controller, based on the internal model principle to reject the disturbances, is considered as follows:

$$K(z^{-1},\theta) = [K_0(z^{-1}) + \theta K_1(z^{-1})]M(z^{-1},\theta) \qquad (10)$$

where K_0 and K_1 are FIR filters of order n and

$$M(z^{-1},\theta) = \frac{1}{1+\theta z^{-1}+z^{-2}} \qquad (11)$$

the disturbance model for a sinusoidal disturbance with frequency $f_1 = \cos^{-1}(-\theta/2)/2\pi$. In order to improve the transient response, the infinity norm of the transfer function between the disturbance and the output, MG_1S, should be minimized. However, since the primary path model G_1 cannot be used in the benchmark, it is replaced by a constant gain. On the other hand, in order to increase the robustness and prevent the activity of the command input at frequencies where the gain of the secondary path is low, the infinity norm of the input sensitivity function $\|KS\|_\infty$ should be decreased as well. Another constraint on the maximum of the modulus of the sensitivity function $\|S\|_\infty < 2$ (6dB) is also considered according to the benchmark requirements (not to amplify the noise at other frequencies).

A gain-scheduled controller is designed using the following steps:

1. Because of very high resonance modes in the secondary path model, a very fine frequency grid with a resolution of 0.5 rad/s (5027 frequency points) is considered.
2. The interval of the disturbance frequencies is divided to 46 points (a resolution of 1Hz), which corresponds to 46 points in the interval $[-1.8478\,,\,-1.4686]$ for the scheduling parameter θ.
3. The following optimization problem is solved:

$$\begin{aligned}
&\min \gamma \\
&\gamma^{-1}\left[|M(e^{-j\omega_k},\theta_i)| + |K(e^{-j\omega_k},\rho(\theta_i))|\right] \\
&\times [1 + L_d(e^{-j\omega_k},\theta_i)]| - \\
&R_e\{[1 + L_d(e^{j\omega_k},\theta_i)][1 + L(e^{-j\omega_k},\rho(\theta_i))]\} < 0, \\
&\\
&0.5|[1 + L_d(e^{-j\omega_k},\theta_i)]| - \\
&R_e\{[1 + L_d(e^{j\omega_k},\theta_i)][1 + L(e^{-j\omega_k},\rho(\theta_i))]\} < 0, \\
&\text{for } k = 1,\ldots,5027, \quad i = 1,\ldots,46
\end{aligned} \qquad (12)$$

where the first constraint is the convexification of $\||MS|+|KS|\|_\infty < \gamma$ and the second constraint that of $\|S\|_\infty < 2$. This is a convex optimization problem for fixed γ and can be solved by an iterative bisection algorithm.

Remarks:

- The controller order (the order of the FIR models for K_0 and K_1 in (10)) is chosen equal to 10 (the controller order is increased gradually to obtain acceptable results). Note that it is much less than the order of the plant model, which is equal to 26.
- The desired open-loop transfer functions are chosen as $L_d(\theta_i) = K_{ini}(\theta_i)G_2$, where $K_{ini}(\theta_i)$ are stabilizing controllers computed by pole placement technique.
- The Frequency-Domain Robust Control Toolbox [11] is used for solving this problem. For the convenience, the internal model is considered as a part of the plant model, i.e. $G(\theta) = M(\theta)G_2$, and after the controller design it is returned to the controller.
- After 7 iterations for the bisection algorithm $\gamma_{\min} = 1.68$ is obtained. The total computation time is about 11 minutes on a personal computer (16GB of DDR3 RAM memory at 1600MHz and processor Intel Core i7 running at 3.4GHz).

The parameters of the final designed gain-scheduled

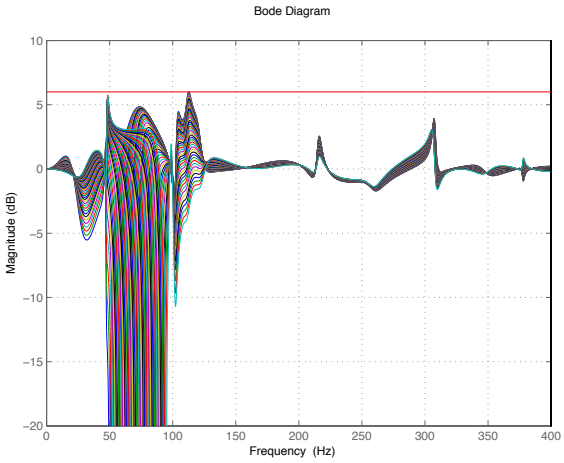

Figure 3: Magnitude plot of the output sensitivity functions for disturbance frequencies from 50Hz to 95Hz

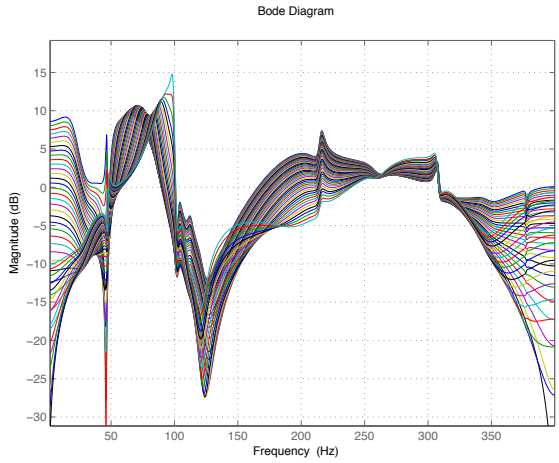

Figure 4: Magnitude plot of the input sensitivity functions for disturbance frequencies from 50Hz to 95Hz

controller in (10) are given by:

$$\begin{aligned} K_0(z^{-1}) &= 3.669 - 2.311z^{-1} - 0.7776z^{-2} \\ &\quad +0.7171z^{-3} + 3.424z^{-4} - 5.402z^{-5} \\ &\quad +5.077z^{-6} - 5.143z^{-7} + 4.637z^{-8} \\ &\quad -2.01z^{-9} + 0.5125z^{-10} \\ K_1(z^{-1}) &= 2.241 - 1.293z^{-1} - 0.7633z^{-2} \\ &\quad +0.4309z^{-3} + 2.673z^{-4} - 3.921z^{-5} \\ &\quad +3.117z^{-6} - 2.638z^{-7} + 2.476z^{-8} \\ &\quad -1.15z^{-9} + 0.3444z^{-10} \end{aligned}$$

This gain-scheduled controller gives very good transient performance and satisfies the constraint on the maximum modulus of the sensitivity function for all values of the scheduling parameter. Figure 3 and Fig. 4 show the magnitude of the output sensitivity functions S and the input sensitivity functions KS, respectively, for 46 gridded values of the disturbance frequencies. One can observe very good attenuation at the disturbance frequencies and the satisfaction of the modulus margin of at least 6dB for all disturbances.

3.2. Controller design for Level 2

In this level of the benchmark, two sinusoidal disturbances should be rejected. The structure of the gain scheduled controller is given by (z^{-1} is omitted):

$$K(\theta_1, \theta_2) = (K_0 + \theta_1 K_1 + \theta_2 K_2) M(\theta_1, \theta_2) \qquad (13)$$

where K_0, K_1 and K_2 are 8th order FIR filters and

$$M(\theta_1, \theta_2) = \frac{1}{1 + \theta_1 z^{-1} + \theta_2 z^{-2} + \theta_1 z^{-3} + z^{-4}} \qquad (14)$$

By considering a hard constraint on the magnitude of the sensitivity function $\|(1 + KG_2)^{-1}\|_\infty < 2.24$ (7dB) the optimization becomes infeasible. Therefore, the following constraint is considered for optimization:

$$|M(1+KG_2)^{-1}| + |(1+KG_2)^{-1}| < \gamma \quad \forall\omega, \forall\theta_1, \forall\theta_2 \quad (15)$$

where γ is minimized. The first term on the left hand side represents the approximation of the disturbance path impulse response (ignoring the unknown transfer function G_1). By minimizing its ∞-norm, we indirectly reduce the transient time (with a tradeoff between fast response and robustness guarantee, coming from the second term).

Since we have two scheduling parameters a resolution of 1Hz for each sinusoidal disturbances leads to $46^2/2 = 1058$ grid points. This increases by a factor of 23 the number of constraints with respect to that of Level 1. Moreover the resolution of the frequency grid is improved from 0.5 rad/s to 0.2 rad/s which increases the number of constraints. The number of variables is also increased from 22 (the coefficients of two FIR of order 10) to 27 (the coefficients of three FIR of order 8). In order to obtain a faster optimization problem, the scenario approach is used. From the set of 1058 frequency pairs, 50 samples are chosen randomly and the constraints are considered just for these frequencies. The stability of the closed-loop system however, is verified a posteriori for all 1058 frequency pairs, which makes the probability of stability constraint violation (between the grid points) very low. The computed controller, however, destabilized the real system for disturbance frequency pair (50-70)Hz. The main reason is the modeling error for the secondary path model around 50Hz. Therefore, a new model for the secondary path provided by the benchmark organizers with smaller modeling error around 50Hz is used for the controller design. A new controller is designed using the scenario approach and achieves $\gamma_{\min} = 10.62$ after 11 iterations with a total computation time of about 15 minutes.

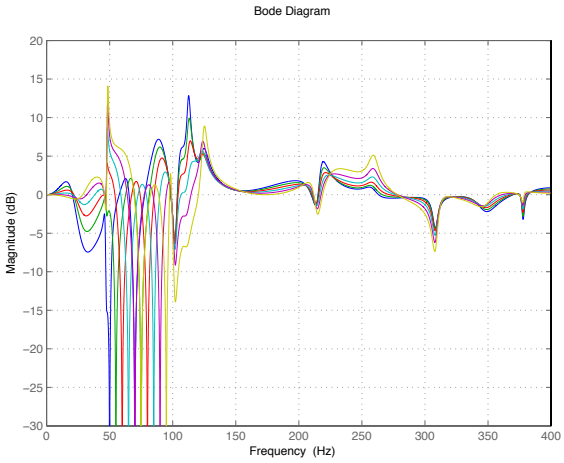

Figure 5: Magnitude of the output sensitivity functions for known disturbance frequencies in $\mathcal{F}$

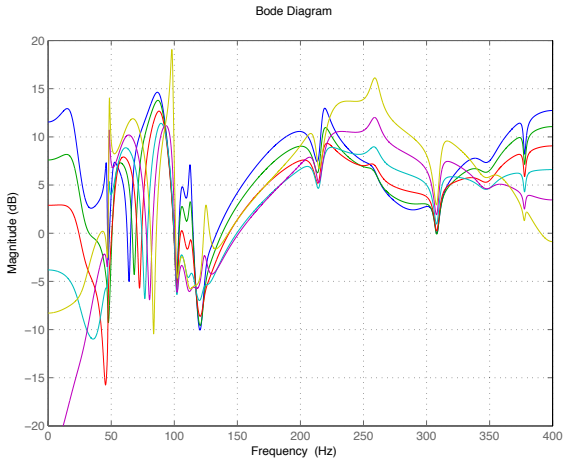

Figure 6: Magnitude of the input sensitivity functions for known disturbance frequencies in $\mathcal{F}$

The controller parameters are:

$$K_0(z^{-1}) = -4.835 + 43.93z^{-1} - 98.74z^{-2} + 96.2z^{-3} \\ -0.3158z^{-4} - 100.8z^{-5} + 117.5z^{-6} - 64.79z^{-7} + 16.35z^{-8}$$

$$K_1(z^{-1}) = -24.02 + 122.4z^{-1} - 226.7z^{-2} + 204.9z^{-3} \\ -52.21z^{-4} - 71.05z^{-5} + 80.54z^{-6} - 36.53z^{-7} + 8.671z^{-8}$$

$$K_2(z^{-1}) = -16.05 + 77.44z^{-1} - 139.6z^{-2} + 124.7z^{-3} \\ -37.19z^{-4} - 28.47z^{-5} + 31.64z^{-6} - 11.83z^{-7} + 2.561z^{-8}$$

Figure 5 and Fig. 6 show the magnitude of the output and input sensitivity functions for *known* disturbance frequencies taken from the following set:

$$\mathcal{F} = \{(50, 70), (55, 75), (60, 80), (65, 85), (70, 90), (75, 95)\}$$

The attenuation of at least 40 dB is obtained for all frequencies but the maximum of the output sensitivity function is greater than 7 dB in some frequencies.

3.3. Controller design for Level 3

Although very good results can be obtained for linear controller design for every triplet disturbance frequencies, a simple gain-scheduled controller that satisfies all constraints could not by obtained by the proposed approach. In fact the optimization problem becomes infeasible for affine dependence of the controller parameters to the scheduling ones and with relaxing the constraints the resulting stabilizing controller does not lead to good performance even for known disturbance frequencies.

It is important to emphasize that there is no theoretical limitation for having three or even more disturbance frequencies. However, increasing the number of frequencies increases the complexity of the optimization problem such that a feasible solution could not be find in the first trials. This problem could be fixed by designing better initial controllers for each fixed frequency and use these controllers for computing L_d, as well by the better choice of the basis functions. However, because of the deadline for the benchmark, the authors decided just to participate in the first and the second level.

3.4. Estimator design

The scheduling parameter θ used in the internal model of disturbance in (11) is estimated using a parameter adaptation algorithm. To estimate the parameters of the disturbance model, we need to measure the disturbance signal $p(t)$ (see Fig. 2). If we model $p(t)$ as the output of an ARMA model with white noise as input, we have:

$$D_p(q^{-1})p(t) = N_p(q^{-1})e(t), \tag{16}$$

where $e(t)$ is a zero mean white noise with unknown variance. Estimation of the parameters of N_p and D_p could be performed by the standard *Recursive Extended Least Squares* method [13], if $p(t)$ was measured. Since $p(t)$ is not available, it is estimated using the measured signal $y(t)$ and the known model of the secondary path. From Fig. 2, we have:

$$p(t) = y(t) - \frac{q^{-d}B(q^{-1})}{A(q^{-1})}u(t) - v_2(t), \tag{17}$$

where $\dfrac{q^{-d}B(q^{-1})}{A(q^{-1})}$ is the parametric model of the secondary path G_2. Since $v_2(t)$ is a zero mean noise signal, unbiased estimate of $p(t)$ is given as

$$\bar{p}(t) = y(t) + [A(q^{-1}) - 1][y(t) - \bar{p}(t)] - B(q^{-1})u(t-d)$$

For the asymptotical rejection of sinusoidal disturbance, there is no need to identify the whole model of the disturbance path, i.e. HG_1 as shown in Figure 2. The information needed is just the frequency of the disturbance. So, by setting $D_p(q^{-1},\theta) = 1 - \theta q^{-1} + q^{-2}$ (for Level 1) and $N_p(q^{-1}) = 1 + c_1 q^{-1} + c_2 q^{-2}$, a simple parameter estimation algorithm can be developed. Let us define :

$$
\begin{aligned}
z(t+1) &= \bar{p}(t+1) + \bar{p}(t-1) && (18)\\
\psi^T(t) &= [-\bar{p}(t), \varepsilon(t), \varepsilon(t-1)]^T && (19)\\
\Theta^T(t) &= [\theta, c_1, c_2]^T && (20)
\end{aligned}
$$

where $\varepsilon(t) = z(t) - \hat{z}(t)$ is the *a posteriori* prediction error. Now, the following recursive adaptation algorithm can be used to estimate the the scheduling parameter θ:

$$
\begin{aligned}
\varepsilon^\circ(t+1) &= z(t+1) - \hat{\Theta}(t)\psi(t)\\
\varepsilon(t+1) &= \frac{\varepsilon^\circ(t+1)}{1 + \psi_f^T(t)F(t)\psi_f(t)}\\
\hat{\Theta}(t+1) &= \hat{\Theta}(t) + F(t)\psi_f(t)\varepsilon(t+1) && (21)\\
F(t+1) &= \frac{1}{\lambda_1(t)}\left[F(t) - \frac{F(t)\psi_f^T(t)\psi_f(t)F(t)}{\frac{\lambda_1(t)}{\lambda_2(t)} + \psi_f^T(t)F(t)\psi_f(t)}\right]
\end{aligned}
$$

where $\psi_f(t) = \frac{1}{N_p(q^{-1})}\psi(t)$, $\varepsilon^\circ(t)$ is the *a priori* prediction error and $\lambda_1(t)$ and $\lambda_2(t)$ define the variation profile of the adaptation gain $F(t)$. Filtered observation vector $\psi_f(t)$ is used to ensure the stability and convergence properties of the adaptation algorithm ([13]). The other condition for the convergence, namely the richness of excitation, is satisfied as long as disturbance is not zero. A constant trace algorithm [13] is used for the adaptation gain.

The same recursive adaptation algorithm is used for Level 2 of the benchmark with the difference that the order of the disturbance model and consequently the number of the scheduling parameters is increased (θ is replaced by a vector $[\theta_1\ ,\ \theta_2]$).

4. Simulation and experimental results

The simulation results are presented for three different tests of each benchmark level: simple step test, step changes in frequencies test and chirp test, according to the benchmark requirements.

4.1. simple step test

The simulation and experimental results for Level 1 are given in Table 1 and Table 2, respectively. The first column gives the global attenuation in dB. It is the ratio of the energy of the disturbance in open-loop to that in closed-loop computed in steady state (last three seconds of the experiment). The second column shows the attenuation at the disturbance frequency. The maximum amplification of the disturbance at other frequencies is computed and shown in the third column together with the frequency at which it occurs. The two-norm of the transient response of the residual force is given in the forth column and the two norm at the steady state (last three seconds) in the fifth column. The peak value of the transient response is given in the 6-th column, and a Benchmark Satisfaction Index (BSI) for the transient duration in the 7-th column (100% means that the transient duration is less than 2 sec. and 0% corresponds to more than 4 sec). The results show more or less good coherence between the simulation and experimental results. Certain discrepancy between the simulation and experimental results for the disturbance frequency of 50Hz probably comes from the modeling error of the secondary-path model, around this frequency, used in the simulator of the benchmark.

The simulation results for simple step test of Level 2 are given in Table 3 and the experimental results in Table

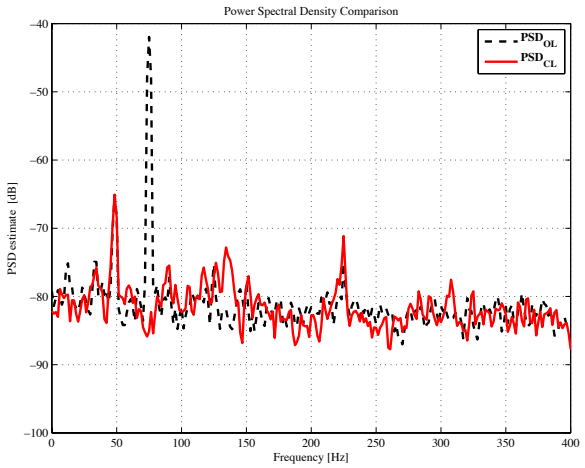

Figure 9: Power spectral density for the real-time simple step test with disturbance frequency of 75Hz (Level 1)

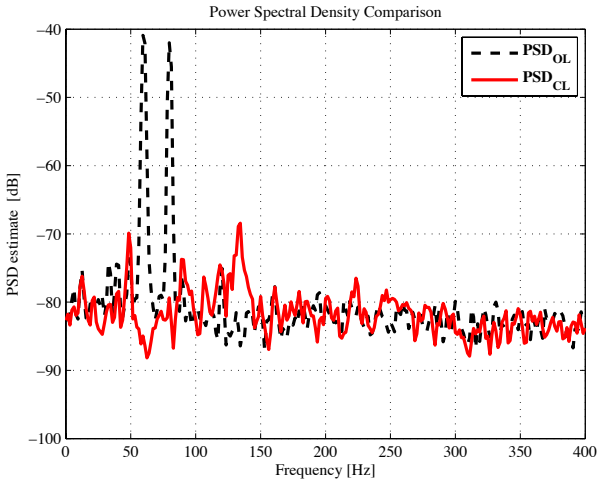

Figure 10: Power spectral density for the real-time simple step test with disturbance frequencies of 60 and 80Hz (Level 2)

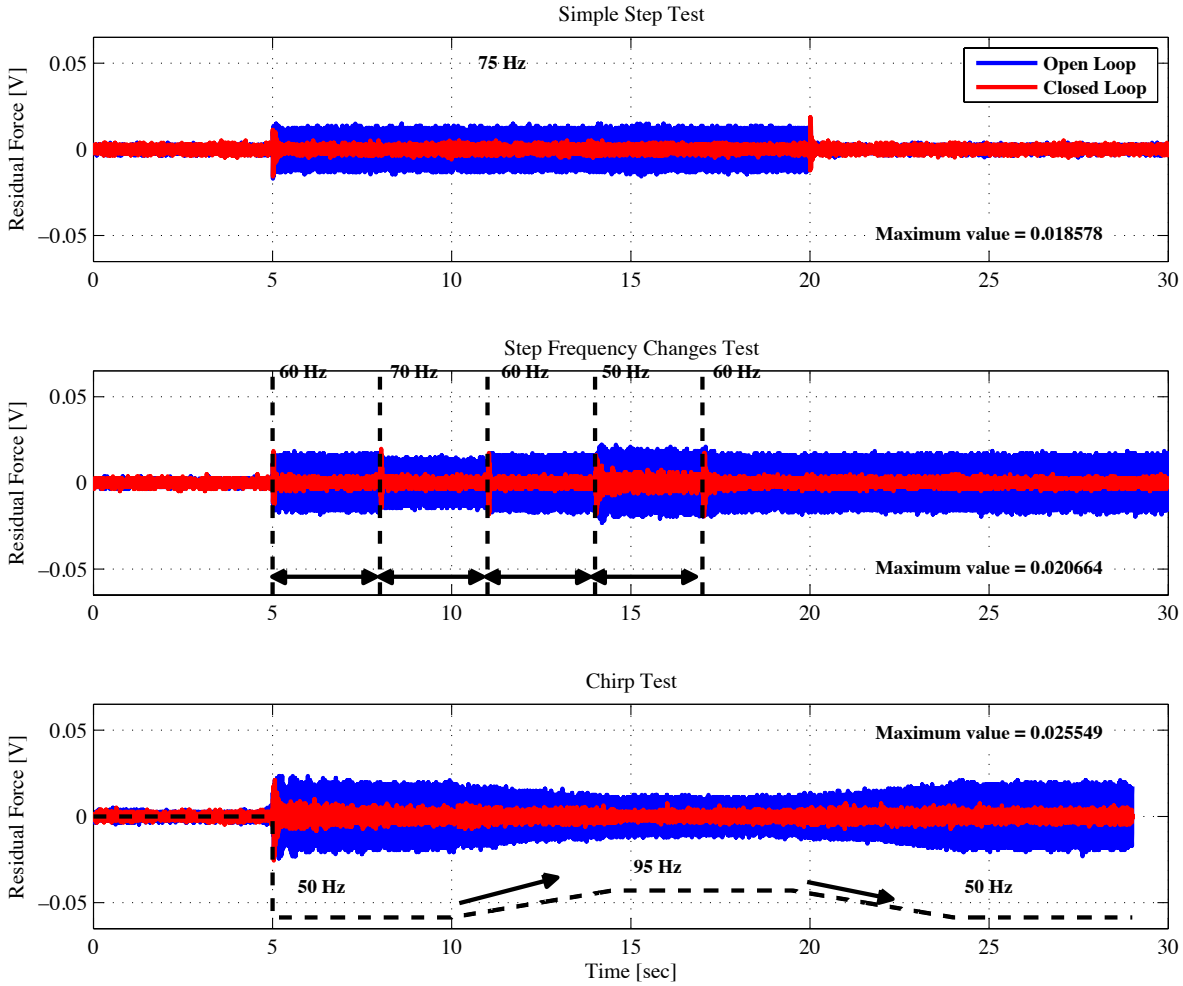

Figure 7: Experimental time-domain responses for different Level 1 tests

Table 1: Simple step test (Simulation) - Level 1

Frequency (Hz)	**Global (dB)**	**Dist. Atte. (dB)**	**Max. Amp. (dB@Hz)**	**Norm^2 Trans. ($\times 10^{-3}$)**	**Norm^2 Res. ($\times 10^{-3}$)**	**Max. Val. ($\times 10^{-3}$)**	**BSI (%)**
50	30.0539	22.1214	9.6674@ 53.12	13.4803	6.0275	19.2347	100.00
55	33.0839	39.1389	5.7785@ 114.06	11.2054	4.2825	21.5834	100.00
60	32.9298	40.6649	5.2791@78.12	9.1452	4.3614	21.5092	100.00
65	33.1775	39.2777	5.4087@73.43	7.9451	4.3065	19.5405	100.00
70	33.5947	47.4173	4.6449@51.56	7.9827	4.1534	22.6636	100.00
75	34.2959	42.8627	3.6597@ 50.00	8.1354	3.9172	22.5296	100.00
80	34.8302	45.3628	3.8744@50.00	8.0156	3.6393	21.3056	100.00
85	34.5090	43.2440	4.0071@50.00	8.6001	3.6477	23.4386	100.00
90	32.3077	39.3682	4.4651@50.00	12.5930	3.8676	25.5074	100.00
95	23.9978	23.8150	4.9679@50.00	15.5999	4.4858	29.8633	100.00

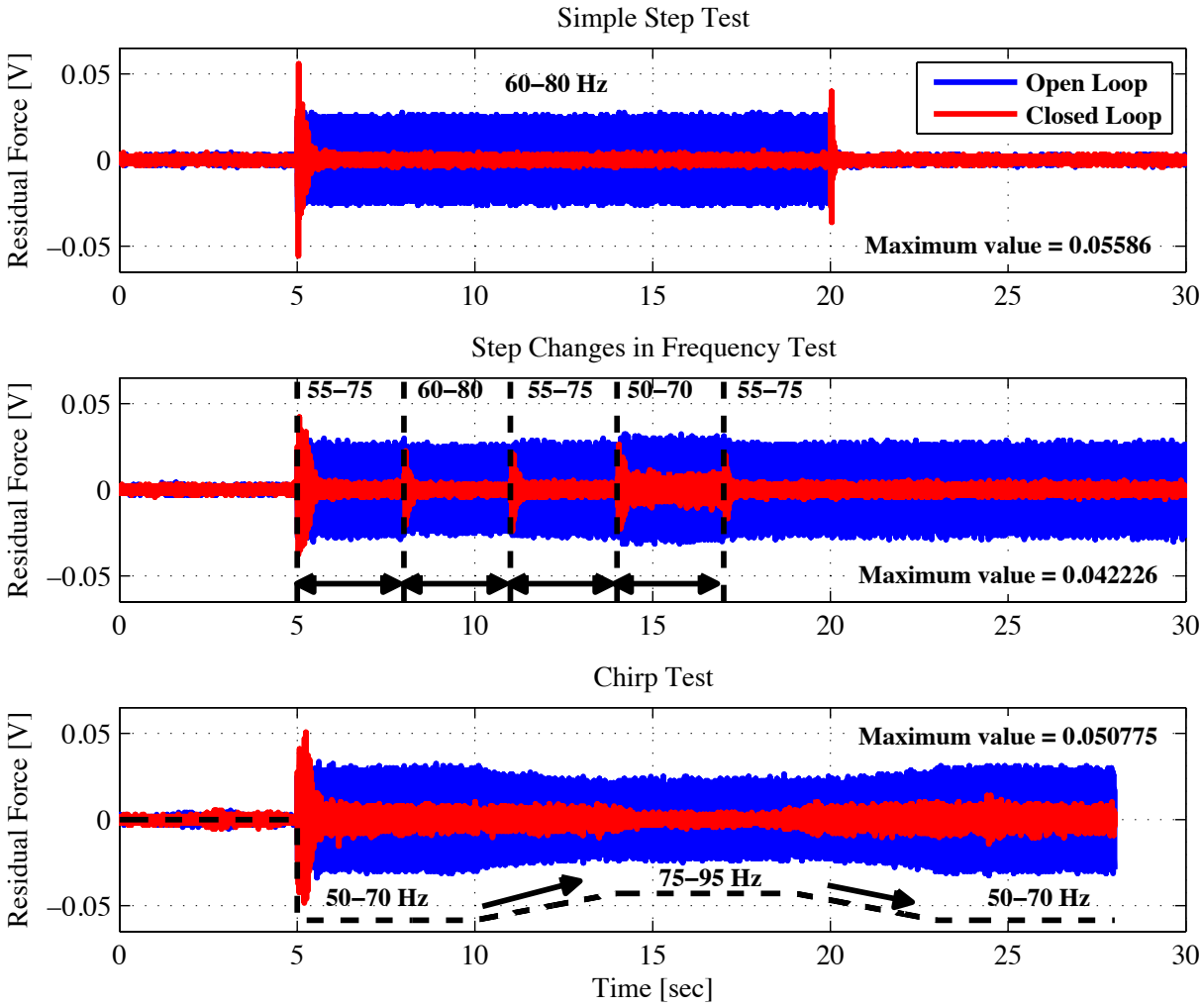

Figure 8: Experimental time-domain responses for different Level 2 tests

Table 2: Simple step test (Experimental results) - Level 1

Frequency (Hz)	Global (dB)	Dist. Atte. (dB)	Max. Amp. (dB@Hz)	Norm^2 Trans. ($\times 10^{-3}$)	Norm^2 Res. ($\times 10^{-3}$)	Max. Val. ($\times 10^{-3}$)	BSI (%)
50	32.1963	26.0390	13.19@117.19	28.7275	9.8031	22.2959	83.88
55	32.9624	41.5091	11.66@125.00	13.7586	5.6248	18.5939	100.00
60	33.7955	41.3196	11.59@70.31	9.9979	5.1623	17.3711	97.99
65	32.5293	45.4435	9.54@134.37	9.8304	5.0178	19.3765	100.00
70	30.0156	42.6926	11.41@134.37	9.3400	5.5506	20.6127	95.06
75	30.9359	43.1902	9.74@137.50	7.7819	4.4682	15.7354	100.00
80	29.6325	44.9083	9.43@137.50	8.5284	5.0297	21.8171	100.00
85	28.3826	38.3824	7.63@118.75	8.0995	5.7268	20.5997	100.00
90	28.2388	37.0264	10.02@135.94	8.8059	5.0778	23.0987	100.00
95	28.8061	37.0992	7.36@114.06	8.5047	4.6892	22.2701	100.00

4. For Level 1 tests, apart from the disturbance at 50Hz, disturbances at other frequencies are rejected. The global attenuation of more than 30 dB is met in simulation for all frequencies. However, in real experiments the performance for the disturbance frequency pair (50-70)Hz is not good. The main reason is that the estimated parameters in the adaptation algorithm do not converge to the true values (a linear controller with known disturbance frequencies performs very well in simulation as well as in real experiments). For the other disturbance frequencies the transient behaviour in simulation and experimental results are close and satisfy more or less the specifications.This effect can be reduced by adding a small damping to the internal model of the disturbance. This way, a small error in the scheduling parameters will have less effect in the performance, but with the cost of having less attenuation for the exact parameter estimates.

Although the maximum amplification of disturbance in simulation is close to that of linear controller, higher values are obtained in real experiments. This probably comes from the modeling error around 129-137 Hz.

The real-time response from the simple step test with disturbance frequency of 75Hz is shown in the first plot of Fig. 7. Similarly, in Fig. 8 the first plot presents the simple step test response for Level 2 with disturbance frequencies of 60 and 80Hz. Figure 9 illustrates the comparison between the open-loop (dashed) and the closed-loop power spectral density for the real-time simple step test with single disturbance frequency of 75Hz. Strong attenuation (around 45dB) at 75Hz and low (or no) amplification at other frequencies can be observed. Similar conclusion can be drawn from Fig. 10 for the simple step test of Level 2 with disturbance frequencies of 60 and 80Hz.

4.2. Step changes in frequencies test

For Level 1 of the benchmark, three sequences of step changes in the frequency of the disturbance are considered. These sequences are defined as follows:

Sequence 1 : $60 \rightarrow 70 \rightarrow 60 \rightarrow 50 \rightarrow 60$
Sequence 2 : $75 \rightarrow 85 \rightarrow 75 \rightarrow 65 \rightarrow 75$
Sequence 3 : $85 \rightarrow 95 \rightarrow 85 \rightarrow 75 \rightarrow 85$

Similarly, for Level 2, two sequences of the step changes in the disturbance frequencies are defined (see the first column of Table 5). The transient performance in simulation for Level 1 and Level 2 are given in Table 5 and the experimental results in Table 6. It can be observed that good performance is obtained for all disturbance frequency pairs except for (50-70) in the real experiment.

The second plot of Fig. 7 and 8 present the real-time response for the first disturbance frequency sequence of the step changes in frequencies test for Level 1 and for Level 2, respectively.

4.3. Chirp test

For Level 1 of the benchmark a chirp signal that starts from 50Hz and goes to 95Hz and returns to 50Hz with a

Table 5: Step changes in frequencies test (Simulation)

	SEQUENCE - 1		
Level 1	**Frequency (Hz)**	**Norm^2 Trans.** ($\times 10^{-3}$)	**Max. Val.** ($\times 10^{-3}$)
	60→70	7.9407	20.7565
	70→60	8.3077	16.5109
	60→50	10.2125	13.4903
	50→60	7.3136	15.6196
	SEQUENCE - 2		
	Frequency (Hz)	**Norm^2 Trans.** ($\times 10^{-3}$)	**Max. Val.** ($\times 10^{-3}$)
	75→85	7.2684	13.9343
	85→75	8.7004	17.0025
	75→65	7.6486	17.0491
	65→75	7.8875	15.2766
	SEQUENCE - 3		
	Frequency (Hz)	**Norm^2 Trans.** ($\times 10^{-3}$)	**Max. Val.** ($\times 10^{-3}$)
	85→95	8.3668	20.2567
	95→85	9.5780	18.5376
	85→75	7.3373	17.1218
	75→85	8.0514	17.4093
Level 2	**SEQUENCE - 1**		
	Frequency (Hz)	**Norm^2 Trans.** ($\times 10^{-3}$)	**Max. Val.** ($\times 10^{-3}$)
	[55-75] → [60-80]	10.0628	22.8093
	[60-80] → [55-75]	16.3247	21.5839
	[55-75] → [50-70]	20.0613	18.7106
	[50-70] → [55-75]	10.0798	17.8500
	SEQUENCE - 2		
	Frequency (Hz)	**Norm^2 Trans.** ($\times 10^{-3}$)	**Max. Val.** ($\times 10^{-3}$)
	[70-90] → [75-95]	11.5762	18.1048
	[75-95] → [70-90]	13.9285	22.5232
	[70-90] → [65-85]	12.0298	23.1736
	[65-85] → [70-90]	10.8733	20.8162

Table 3: Simple step test (Simulation) - Level 2

Frequency (Hz)	**Global (dB)**	**Dist. Atte. (dB)-(dB)**	**Max. Amp. (dB@Hz)**	**Norm^2 Trans.** ($\times 10^{-3}$)	**Norm^2 Res.** ($\times 10^{-3}$)	**Max. Val.** ($\times 10^{-3}$)	**BSI (%)**
50-70	35.5110	27.42 - 23.00	11.28@114.06	87.6744	6.4925	61.5624	100.00
55-75	38.6182	33.68 - 33.59	9.59@114.06	67.8341	4.6086	59.1878	100.00
60-80	39.8107	41.80 - 37.09	6.84@114.06	53.7933	3.9936	53.7369	100.00
65-85	39.9478	49.57 - 43.77	6.37@50.00	64.8855	3.8930	68.9495	100.00
70-90	38.4478	54.70 - 47.07	9.09@50.00	80.7946	4.2437	76.4654	100.00
75-95	35.1036	48.74 - 36.81	11.17@50.00	95.3054	4.7593	72.0523	100.00

Table 4: Simple step test (Experimental results) - Level 2

Frequency (Hz)	**Global (dB)**	**Dist. Atte. (dB)-(dB)**	**Max. Amp. (dB@Hz)**	**Norm^2 Trans.** ($\times 10^{-3}$)	**Norm^2 Res.** ($\times 10^{-3}$)	**Max. Val.** ($\times 10^{-3}$)	**BSI (%)**
50-70	24.6660	20.58 - 17.49	18.06@131.25	144.4955	34.0463	50.7286	100.00
55-75	36.9297	34.20 - 30.54	18.88@129.69	174.1515	6.4665	86.2932	100.00
60-80	39.9376	44.32 - 37.43	18.00@134.37	64.0941	4.0669	55.8595	100.00
65-85	32.5931	37.85 - 32.34	14.65@ 135.94	47.4775	8.2762	54.6568	100.00
70-90	36.3403	55.54 - 47.05	14.41@ 137.50	52.3746	4.7614	63.1648	100.00
75-95	33.7952	43.26 - 36.27	13.07@ 137.50	116.2289	5.7348	86.3334	50.78

variation rate of 10 Hz/sec is applied as the disturbance signal. For Level 2 the disturbance frequencies change from (50-70)Hz to (75-95)Hz with a variation rate of 5 Hz/sec and return to (50-70)Hz. The maximum value and the two-norm of the disturbance response in simulation and in the real-time experiment are given in Table 7. The experimental results of the chirp disturbance responses for Level 1 and Level 2 are given in Fig. 7 and 8, respectively.

5. Conclusions

A new method for fixed-order gain-scheduled H_∞ controller design is proposed and applied to the active suspension benchmark. It is shown that one or two unknown sinusoidal disturbances can be rejected using the gain-scheduled controller and an adaptation algorithm that estimates the internal model of the disturbance. The proposed gain-scheduled controller design method is able to satisfy all frequency-domain constraints. However, the results are slightly deteriorated in simulation and real experiments. The main reasons are the followings:

- During the convergence of the scheduling parameter, the whole system becomes nonlinear and the desired performance is not achieved.
- Even at the steady state, there is always an estimation error in the scheduling parameter.
- The modeling error in the secondary-path model is not considered in the design.

Although the proposed method could consider the modeling error in the design, it has not been taken to account for some reasons. First, it was supposed that the provided model for the benchmark is very close to the real system and modeling error can be neglected. Second, considering the unmodelled dynamics makes the optimization method more complicated (number of constraints increases) and, finally, robust controllers lead generally to conservative solutions to the detriment of performance.

Acknowledgment

The authors would like to thank Prof. Landau for his advices and good discussions and Abraham Castellanos Silva for his help and support during the real-time experiments.

References

[1] A. Sacks, M. Bodson, P. Khosla, Experimental results of adaptive periodic disturbance cancelation in a high performance magnetic disk drive, ASME Journal of Dynamic Systems Measurement and Control 118 (1996) 416–424.

[2] M. Bodson, Rejection of periodic disturbances of unknown and time-varying frequency, International Journal of Adaptive Control and Signal Processing 19 (2005) 67–88.

[3] G. Calafiore, M.C. Campi, The scenario approach to robust control design, IEEE Transactions on Automatic Control 51 (2006) 742–753.

[4] C.J. Doyle, B.A. Francis, A.R. Tannenbaum, Feedback Control Theory, Mc Millan, New York, 1992.

[5] P. Gahinet, P. Apkarian, A linear matrix inequality approach to H_∞ control, International Journal of Robust and Nonlinear Control 4 (1994) 421–448.

[6] G. Galdos, A. Karimi, R. Longchamp, Robust controller design by convex optimization based on finite frequency samples of spectral models, in: 49th IEEE Conference on Decision and Control, Atlanta, USA.

[7] H. Du, L. Zhang, Z. Lu, X. Shi, LPV technique for the rejection of sinusoidal disturbance with time-varying frequency, IEE Proceedings - Control Theory and Applications 150 (2003) 132–138.

Table 6: Step changes in frequencies test (Experimental results)

Level 1	**SEQUENCE - 1**		
	Frequency (Hz)	**Norm^2 Trans.** ($\times 10^{-3}$)	**Max. Val.** ($\times 10^{-3}$)
	60→70	9.8243	19.7289
	70→60	9.8454	18.2445
	60→50	22.6091	18.2210
	50→60	13.8104	19.4511
	SEQUENCE - 2		
	Frequency (Hz)	**Norm^2 Trans.** ($\times 10^{-3}$)	**Max. Val.** ($\times 10^{-3}$)
	75→85	8.5829	15.7833
	85→75	10.1036	17.3218
	75→65	9.9323	19.7391
	65→75	10.1643	19.72531
	SEQUENCE - 3		
	Frequency (Hz)	**Norm^2 Trans.** ($\times 10^{-3}$)	**Max. Val.** ($\times 10^{-3}$)
	85→95	8.5971	15.8359
	95→85	9.8947	17.2523
	85→75	9.1527	16.0698
	75→85	9.1745	17.0129
Level 2	**SEQUENCE - 1**		
	Frequency (Hz)	**Norm^2 Trans.** ($\times 10^{-3}$)	**Max. Val.** ($\times 10^{-3}$)
	[**55-75**] → [**60-80**]	13.7017	22.5980
	[**60-80**] → [**55-75**]	18.0644	23.9297
	[**55-75**] → [**50-70**]	51.0763	26.2669
	[**50-70**] → [**55-75**]	14.2444	20.1445
	SEQUENCE - 2		
	Frequency (Hz)	**Norm^2 Trans.** ($\times 10^{-3}$)	**Max. Val.** ($\times 10^{-3}$)
	[**70-90**] → [**75-95**]	13.0523	18.9047
	[**75-95**] → [**70-90**]	12.7703	21.6059
	[**70-90**] → [**65-85**]	15.5371	20.3018
	[**65-85**] → [**70-90**]	13.3272	18.9160

Table 7: Chirp Changes

	Error	
	Maximum Value ($\times 10^{-3}$)	**Mean Square Value** ($\times 10^{-6}$)
Level 1 - Sim	6.40	3.5910
Level 1 - Exp	7.54	4.5412
Level 2 - Sim	10.12	10.5170
Level 2 - Exp	11.56	11.8759

[8] I. D. Landau, A. Constantinescu, D. Rey, Adaptive narrow band disturbance rejection applied to an active suspension - an internal model principle approach, Automatica 41 (2005) 563–574.

[9] I. D. Landau, T. B. Airimitoaie, A. C. Silva, Gabriel Buche, An active vibration control system as a benchmark on adaptive regulation, in: Submitted to European Control Conference, Zurich, Switzerland. URL: `http://www.gipsa-lab.grenoble-inp.fr/~ioandore.landau/benchmark_adaptive_regulation`.

[10] K. K. Chew, M. Tomizuka, Digital control of repetitive errors in disk drive systems, in: American Control Conference, Pittsburgh, PA, USA, pp. 540–548.

[11] A. Karimi, Frequency-domain robust controller design: A toolbox for MATLAB, 2012. URL: `http://la.epfl.ch/FDRC_Toolbox`.

[12] A. Karimi, G. Galdos, Fixed-order H_∞ controller design for nonparametric models by convex optimization, Automatica 46 (2010) 1388–1394.

[13] I.D. Landau, R. Lozano, M. M'Saad, A. Karimi, Adaptive Control: Algorithms, Analysis and Applications, Springer-Verlag, London, 2011.

[14] M. Bodson, A. Sacks, P. Khosla, Harmonic generation in adaptive feedforward cancelation schemes, IEEE Transactions on Automatic Control 33 (1994) 2213–2221.

[15] P. Mäkilä, Approximation of stable systems by laguerre filters, Automatica 26 (1990) 333–345.

[16] P. Apkarian, P. Gahinet, G. Becker, Self-scheduled H_∞ control of linear parameter-varying systems: a design example, Automatica 31 (1995) 1251–1261.

[17] P. Arcara, S. Bittanti, M. Lovera, Periodic control of helicopter rotors for attenuation of vibrations in forward flight, IEEE Transactions on Control Systems Technology 8 (2000) 883–894.

[18] P. Ballesteros, X. Shu, W. Heins, C. Bohn, LPV gain-scheduled output feedback for active control of harmonic disturbances with time-varying frequencies, in: Advances on Analysis and Control of Vibrations - Theory and Applications, Intechopen.com, Rijeka, Croatia, 2012.

[19] S. M. Kuo, D. R. Morgan, Active noise control systems: Algorithms and DSP implementations, John Wiley & Sons, Inc., New York, NY, USA, 1995.

[20] W. Heins, P. Ballesteros, X. Shu, C. Bohn, LPV gain-scheduled observer-based state feedback for active control of harmonic disturbances with time-varying frequencies, in: Advances on Analysis and Control of Vibrations - Theory and Applications, Intechopen.com, Rijeka, Croatia, 2012.

[21] Z. Emedi, A. Karimi, Fixed-order LPV controller design for rejection of a sinusoidal disturbance with time-varying frequency, in: IEEE Multi-Conference on Systems and Control, Dubrovnik, Croatia.